JOURNAL OF APPLIED ELECTROCHEMISTRY 22 (1992) 140–150

Oxygen reduction on Ru-oxide pyrochlores bonded to a proton-exchange membrane

J.-M. ZEN, R. MANOHARAN, J. B. GOODENOUGH

Center for Materials Science and Engineering, ETC 5.160, University of Texas at Austin, Austin, TX 78712-1084, U.S.A.

Received 31 January 1991; revised 8 April 1991

Oxygen reduction at a gas-fed, porous, ruthenium-pyrochlore electrode attached to a Dow Developmental Fuel Cell Membrane was measured in solutions of various pH. Electrode assemblies containing high surface area $Pb_2Ru_{2-x}Pb_xO_{7-y}$ or $Bi_2Ru_{2-x}Bi_xO_{7-y}$ with different amounts of Teflon content with/without the incorporation of Dow gel in the active part of the electrode with/without a CO_2-treated Vulcan XC-72 carbon substrate were tested. The oxide pyrochlores were found to be chemically stable and to show their lowest overpotential if separated from a 2.5 M H_2SO_4 proton reservoir by the membrane. Interesting oxygen reduction activity at room temperature was obtained with the $Pb_2Ru_{1.74}Pb_{0.26}O_{7-y}$ electrode bonded with 22% by weight Teflon and incorporating 5% by weight Dow gel. The performance of the oxides against B-site Pb concentration and a measurement of the surface charge on the particles indicate that, in this configuration, the active sites for the oxygen reduction reaction are OH^- species at the O-site positions of the $A_2B_2O_6O'_{1-y}$ pyrochlores, especially the bridging oxygen with one Ru and one Pb near neighbour, i.e. Pb–O_b–Ru. Evidence that oxide particles precipitated on CO_2-treated carbon transfer electrons to the substrate is also presented.

1. Introduction

Direct hydrocarbon/air fuel cells rely on the four-electron reduction of dioxygen to water at the cathode. To avoid carbonate formation, low-temperature cells use an acid electrolyte. To date the only practical electrocatalyst for the oxygen reduction reaction (ORR) in acid at low temperatures is platinum. The development of a less expensive oxide catalyst for the ORR that is both stable and more active than platinum in acid is, therefore, of considerable technical interest.

The ruthenium-oxide pyrochlores $Pb_2Ru_{2-x}Pb_xO_{7-y}$ and $Bi_2Ru_{2-x}B_xO_{7-y}$ were first identified by Horowitz *et al.* [1] as active catalysts for the ORR in alkaline solution. A previous study [2] has shown that $Pb_2Ru_{2-x}Pb_xO_{7-y}$ is stable in 2.5 M H_2SO_4 solutions for several days, but it corrodes under cathodic load; $Bi_2Ru_{2-x}Bi_xO_{7-y}$ is stable only in solutions of pH > 4.5. One purpose of the present study was to investigate the stability of the ruthenium-oxide pyrochlores under a cathodic load when bonded to a proton-exchange membrane; in these membranes, the anions are immobile.

Proton-exchange membranes such as NAFION® from DuPont and the Dow Developmental Fuel Cell Membrane (hereafter, referred to as the Dow membrane) from the Dow Chemical Company offer a convenient H^+-ion electrolyte for any hydrocarbon/air fuel cell. Both NAFION® and the Dow membrane contain water and perfluorinated sulphonic acid polymers. In an unpressurized cell, the former is stable up to 110° C whereas the latter has been reported to be stable up to ~165–200° C depending on the rate of heating and the equivalent weights of the polymers [3, 4]. We have therefore chosen to investigate the stability and room temperature activity of electrodes containing $Pb_2Ru_{2-x}Pb_xO_{7-y}$ or $Bi_2Ru_{2-x}Bi_xO_{7-y}$ catalysts bonded – either directly or via a treated-carbon substrate – to the Dow membrane.

Previous studies [5, 6] have also presented evidence for a change in the location of the active site on $Pb_2Ru_{2-x}Pb_xO_{7-y}$ for the rate-determining step of the ORR on going from alkaline to acid solution. The $A_2B_2O_6O'_{1-y}$ pyrochlore structure has two types of oxygen; the O oxygen bond to both A and B cations whereas the O′ oxygen bond to only A cations. On variation of the electrolyte pH, a maximum in the overpotential at a current density of 5 mA cm^{-2} occurred at (or near) a pH below which the surface charge $q_s > 0$ of the $Pb_2Ru_{2-x}Pb_xO_6O'_{1-y}$ particles showed a sharp increase with decreasing pH. This correlation was interpreted to indicate a change in the active oxide site for the rate-determining step of the ORR from OH^- species at O′ sites to OH^- species at O sites. A second objective of the present study was to investigate how bonding of the electrode to a proton-exchange membrane influences this shift in the active site and to determine whether the influence improves the activity of the ORR on the oxide for a given pH of an acidic proton source on the opposite side of the membrane.

The assembly of an electrode is a critical part of its performance. We describe the steps used to obtain an optimal, but certainly not the optimum, electrode

0021-891X/92

configuration for testing. We discuss the introduction of Teflon to bind the electrode, the use of CO_2-treated carbon as a substrate for the catalyst, the effect on cell performance of the amount of Pb substituted for Ru in the B sites of the pyrochlore structure, and the incorporation of a Dow gel, a gel made from the Dow membrane*, both to bond the electrode to the membrane and to interpenetrate the carbon substrate with the solid-polymer electrolyte. Moreover, we report measurements of the pH dependence of the charge on the carbon oxide subassemblies; comparison with similar measurements for the oxide particles alone provides indirect information on electron transfer from the oxide to the treated-carbon substrate.

2. Experimental details

2.1. *Electrode preparation*

High-surface-area $Pb_2Ru_{2-x}Pb_xO_{7-y}$ ($x = 0.05$ to 0.4) and $Bi_2Ru_{2-x}Bi_xO_{7-y}$ ($x = 0.4$) were prepared by the precipitation method of Horowitz *et al.* [1]. An appropriate molar ratio of $Pb(NO_3)_2$:$RuCl_3 \cdot 3H_2O$ was dissolved in aqueous solution at 75° C under constant stirring. Approximately 6% KOH was added to the solution so as to maintain a pH of 13; precipitation of the hydroxides was carried out at 75° C under constant stirring and purging of the solution with oxygen gas for 24 h. The filtered product was washed with distilled water until any alkali present was removed; it was then dried in an oven at 130° C. A similar procedure was used to prepare $Bi_2Ru_{2-x}Bi_xO_{7-y}$ except that a much longer reaction time (~4 days) was needed. For some compounds, X-ray powder diffraction gave broad pyrochlore peaks in an amorphous background; heating in air at 300° C for 24 h gave a fairly well crystallized pyrochlore X-ray pattern. The lattice parameters for all the compounds were in good agreement with reported literature values [7].

Following Manoharan [8], gas activation of Vulcan XC-72 carbon was carried out by heating in a CO_2 atmosphere at 900° C for 1 h; this treatment produced a 27% weight loss of carbon. To impregnate the surface of the gas-activated carbon particles with the oxide pyrochlore precipitate, the fine carbon powder was mixed with the aqueous solution of reactants before the hydroxide-precipitation step.

The electrodes were fabricated as follows. Distilled water was added to a measured quantity of either the catalyst precipitate or the catalyst-impregnated carbon powder; a certain amount of 5% (v/v) Dow gel was also added in some preparations. The 5% (v/v) Dow gel was prepared by diluting with water the dissolved Dow polymer, which is in proton form in concentrated ethanol. The mixture was thoroughly homogenized with a sonicator before a dilute Teflon dispersion (DuPont No. T-30 suspension) was added while the mixture was being slightly heated and agitated with a hot plate attached to a magnetic stirrer. The product material was centrifuged and spread onto a Teflon-containing carbon sheet.

The electrode thus formed was bonded to a Dow membrane by placing the Dow membrane on top of the coated surface; the assembly was then hot-pressed at 150° C and 500 p.s.i. unless otherwise specified.

2.2. *Electrochemical measurements*

A pressed electrode was cooled to room temperature and loaded for testing into a half-cell configuration similar to that described elsewhere [9]. The membrane and electrode assembly, with the electrode facing down, were placed between two pieces of the test cell, which were then clamped together. The top half of the cell was used as a reservoir of variable pH to provide a source of protons to be transported through the membrane and consumed in the porous electrode – presumably in the ORR. For most measurements the reservoir was 2.5 M H_2SO_4. The bottom half of the test cell was a hollow cavity with an inlet and outlet used to feed reactant gas, oxygen or nitrogen in this study, to the porous electrode. The electrode area exposed to the electrolyte in this cell was 0.125 cm^{-2}. A Pt gauze was used as the counter electrode, and the reference electrode was Hg/Hg_2SO_4, SO_4^{2-} (2.5 M H_2SO_4), designated MMS, or saturated calomel electrode (SCE).

Steady-state galvanostatic polarization data and cyclic voltammograms were recorded with an EG&G Model 273 potentiostat/galvanostat interfaced to an IBM PxT microcomputer via a National Instruments IEEE-488 General-Purpose Interface (GPIB) card. The EG&G HEADSTART™ Creative Electrochemistry Software was used to drive the measurements, process the data, and display the results.

The EG&G Model 273 was also used to apply a 62.5 Hz, ±50 mV square wave to the cell to measure the uncompensated resistance (R_u). The waveform and rise time of the response current were monitored with an oscilloscope; the R_u value is obtained by adjusting the value of a compensation resistance until the response waveform has the fastest rise time without ringing and rapidly decays to a flat value.

2.3. *P.z.z.p measurement*

The solution pH giving zero charge on an in-solution particle is the point of zero zeta potential (p.z.z.p.); it was determined by potentiometric acid-base titration [10–15]. The oxide powder was suspended in 25 ml of aqueous solution of 0.001 M KOH and 0.1 M KCl. The suspensions were titrated with a pH 1.00 solution (KCl–HCl pH 1.00 buffer solution from Fisher) in the presence of continuous stirring; nitrogen gas was bubbled through the solution to prevent any con-

* Although the Dow gel is made from the Dow membrane, it is not a product of the Dow Chemical Company and may therefore vary in composition from lot to lot, even if supplied by the Dow Chemical Company.

tamination from the CO_2 present in the air. The end point of each titration was determined after the pH reading became stable. Comparison of the titration curve with one obtained for a blank solution permitted determination of the mean surface charge on the oxide particles due to protonation or deprotonation of the surface; the BET surface area of the particles was determined for this calculation.

3. Results

3.1. *Electrochemical stability*

All the $Pb_2Ru_{2-x}Pb_xO_{7-y}$ (x = 0.05 to 0.4) and $Bi_2Ru_{2-x}Bi_xO_{7-y}$ compounds were found to be stable in the test cell where the catalyst was bonded to one side of the Dow membrane and 2.5 M H_2SO_4 solution contacted the other side. On introduction of the 2.5 M H_2SO_4 solution into the cell and oxygen gas from the rear side of the electrode, the open-circuit voltages shifted to a more positive equilibrium potential, indicating the establishment of an ORR at the protonated oxide surface. The rate of shift depended on the oxygen pressure on the rear side of the electrode; the higher the oxygen pressure, the greater the perturbation of the hydrogen-bonded solution layer at the oxide surface.

If lead-ruthenium or lead-iridium oxide pyrochlores are brought into direct contact with 2.5 M H_2SO_4, elemental Pb is reported [5, 6] to be extruded into the surface during the anodic sweep of a cyclic voltammogram (CV) taken from -1 to 1 V/MMS; on the cathodic sweep the surface Pb reacts with the electrolyte to form $PbSO_4$. In the case of membrane-bonded oxides, immobile $-SO_3H^-$ groups bonded to the fluorocarbon skeleton of the membrane replace mobile SO_4^{2-} anions at the oxide surface, but the CV registers no anodic or cathodic current at potentials negative of -0.4 V to indicate the diffusion of Pb^{2+} into or from the perfluorosulphonic acid membrane.

3.2. *Electrode optimization*

The principal factors governing the porous structure of a Teflon-bonded electrode are the amount of Teflon and the method of compaction. The optimum pressing temperature is independent of the Teflon composition over the range 15 to 30% by weight Teflon. In order to determine the optimum pressing temperature, we used initially 25% by weight Teflon in the active layer and varied the hot-pressing conditions while keeping all other parameters constant – *viz.* the Dow membrane, the Teflon-containing carbon sheet, hot-pressing at 500 p.s.i., and an oxygen partial pressure p_{O_2} = 5 cm Hg applied to the reverse side of the electrode. The best polarization curves were obtained for a pressing temperature 140° C $\leqslant T \leqslant$ 155° C; it is difficult to get good binding with $T <$ 135° C, and the Dow membrane appeared to be altered for $T >$ 165° C, which is consistent with reference [4]. The electrode performance was independent of the pressing pressure over the range of 500–1000 p.s.i.; this parameter does not appear to be critical. The optimum Teflon content was then determined for a 2.5 M H_2SO_4 reservoir at room temperature. Figure 1 compares the short-time polarization curves (30 s for each data point) for electrodes of different Teflon content in the active layer and a pressing temperature of 150° C with all other parameters kept the same as in the initial experiments. The overvoltage increases with the amount of inactive Teflon binder, but 15% (w/w of catalyst) Teflon is insufficient to provide the good binding needed for an effective three-phase interface. On the other hand, too much binder (> 25% Teflon by weight) also results in poor performance. The 22% Teflon sample gave the best performance; therefore this amount of Teflon was used for all test electrodes.

Just as incorporation of NAFION® gel with a carbon substrate facilitated binding of an electrode to a NAFION® membrane [16, 17], so also the incorporation of Dow gel into the electrode fabrication facilitates binding of the electrode to a Dow membrane. A

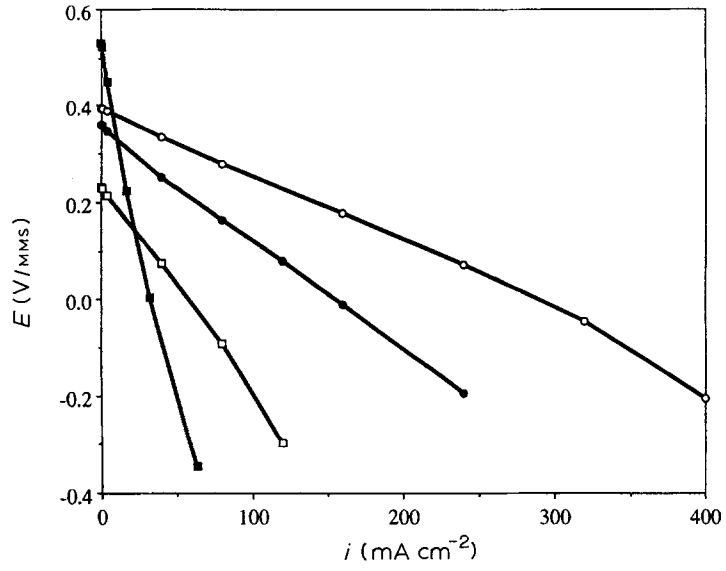

Fig. 1. Effect of Teflon addition on performance for $Pb_2Ru_{1.9}Pb_{0.1}O_{7-y}$ electrodes bonded to a Dow membrane contacting a 2.5 M H_2SO_4 reservoir solution. The data were taken at room temperature with increasing current and 30 s at each data point. Key: (○) 22, (●) 25, (□) 30 and (■) 15%.

unique feature of our electrode preparation was the incorporation of Dow gel in the active layer both to help binding to the Dow membrane and to provide the necessary interface between catalyst, reactant, and electrolyte. With the amount of Teflon in the active mixture fixed at its optimum value of 22% by weight, the amount of Dow gel added was varied from 0.6–9% (w/w) of the oxides. Electrodes containing 5% Dow gel by weight of the oxide gave optimum results.

Varying the oxygen flow rate on the rear side of the electrode from 1 to 20 $cm^3 min^{-1}$ gave no significant change in the measured polarization curve over the current range 0–200 mA cm^{-2}. Increasing the oxygen pressure from 1 to 5 p.s.i. shifted the polarization curve only slightly toward more positive potentials.

3.3. *Electrode performance*

3.3.1. Oxide electrodes. Figures 2–5 show performance data for a $Pb_2Ru_{1.74}Pb_{0.26}O_{7-y}$ electrode with 5% Dow gel incorporated and bonded to a Dow membrane. Fig. 2 presents the chronopotentiograms taken at a constant current density of 5 mA cm^{-2} for various values of the pH of the aqueous-electrolyte reservoir. The pH of the solution reservoir was monitored with an ORION pH meter; it was varied by adding either H_2SO_4 solution or KOH solution to 0.5 M Na_2SO_4. These curves clearly demonstrate (a) that protons from the solution reservoir are transported across the membrane to the porous-electrode structure and (b) that the concentration of H^+ or OH^- species at the electrode/electrolyte interface is strongly influenced by the pH of the solution reservoir outside the membrane. From the flat portion of the potentiograms of Fig. 2, the polarization loss relative to the reversible

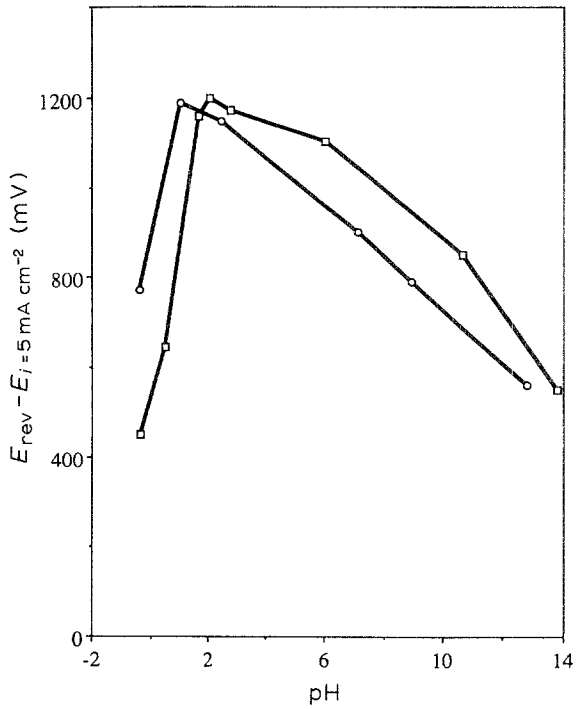

Fig. 3. Variation of low-current-density (5 mA cm^{-2}) overpotential with reservoir pH for a carbon-bonded $Pb_2Ru_{2-x}Pb_xO_{7-y}$ electrode in an aqueous electrolyte. Data from [6] are shown for comparison. (□) $Pb_2Ru_{1.74}Pb_{0.26}O_{7-y}$/ Dow membrane at 25° C (5% Dow gel); (○) $Pb_2Ru_{2-x}Pb_xO_{7-y}$/C at 60° C [6].

potential at a current density of 5 mA cm^{-2} can be obtained as a function of reservoir pH; the result — shown in Fig. 3 — indicates a maximum overpotential near a reservoir pH 2 with a sharp reduction on going to smaller pH. The lowest overpotential occurs at 2.5 M H_2SO_4 (pH ~ -0.37), and all subsequent tests were made with a 2.5 M H_2SO_4 reservoir solution. The shape of the curve can be seen to be similar to that

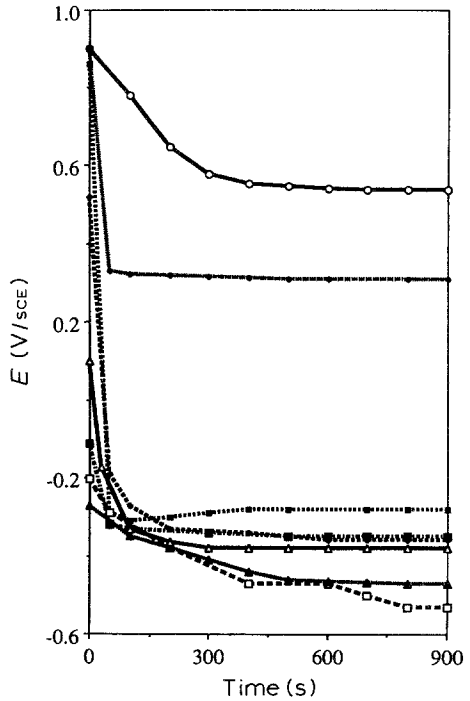

Fig. 2. Room-temperature 5 mA cm^{-2} chronopotentiograms versus reservoir pH for a $Pb_2Ru_{1.74}Pb_{0.26}O_{7-y}$ electrode with 5% Dow gel incorporated and bonded to a Dow membrane. pH: (○) – 0.37, (●) 0.47, (■) 1.65, (○) 2.02, (■) 2.75, (□) 6.00, (▲) 10.68 and (△) 13.8.

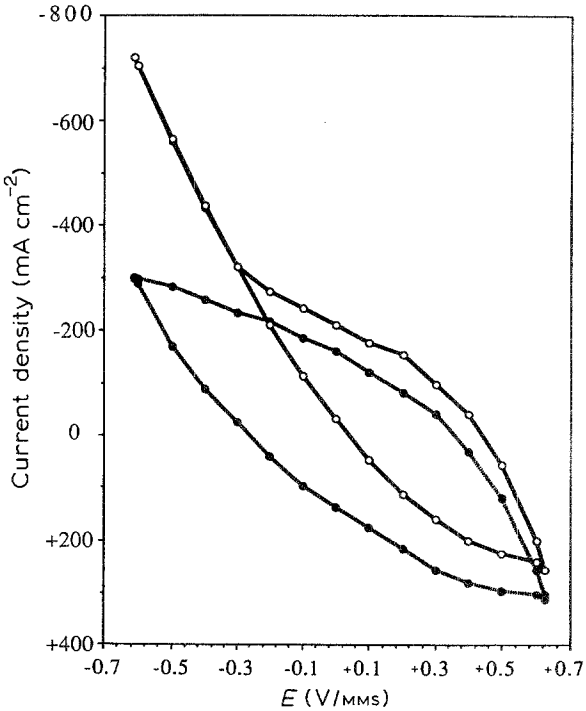

Fig. 4. Room-temperature cyclic voltammograms for a $Pb_2Ru_{1.74}Pb_{0.26}O_{7-y}$ electrode with 5% Dow gel incorporated and bonded to a Dow membrane with a 2.5 M H_2SO_4 reservoir and a scan rate of 25 mV s^{-1}; (○) p_{O_2} = 10 p.s.i., (●) p_{N_2} = 10 p.s.i.

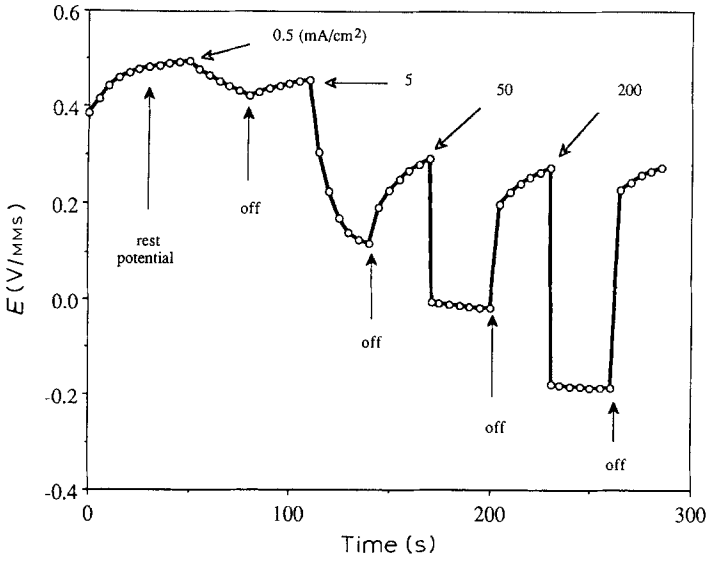

Fig. 5. Room-temperature chonopotentiogram for a $Pb_2Ru_{1.74}Pb_{0.26}O_{7-y}$ electrode with 5% Dow gel incorporated and bonded to a Dow membrane obtained at different current densities with a 2.5 M H_2SO_4 reservoir and a p_{O_2} = 10 p.s.i.

reported for aqueous solutions [6], but shifted to higher pH. Bonding to the Dow membrane effectively lowers the pH of the electrolyte, which results in a significant lowering of the overpotential at 2.5 M H_2SO_4 for the ORR; at these pH values we believe the active site for the rate-determining step is an OH^- species at an O oxygen of the pyrochlore structure [6].

Figure 4 compares room-temperature cyclic voltammograms taken in 10 p.s.i. oxygen and nitrogen on the back side of the $Pb_2Ru_{1.74}Pb_{0.26}O_{7-y}$ electrode with a 2.5 M H_2SO_4 reservoir. These curves clearly show that the ORR is occurring. The current density at $E = -610$ mV/MMS provides a measure of the activity; it decreases with decreasing oxygen pressure to the value shown for the nitrogen curve. Moreover, the activity could be reversibly switched back and forth merely by changing between oxygen and nitrogen gas at the rear side of the electrode.

The room-temperature chronopotentiogram of Fig. 5 shows typical charging curves for the different current densities. On switching off the current, the rest potential always shifted positively toward a constant equilibrium value. The recovery process was rather slow, but the rest potential always came back to its original equilibrium value. The higher the applied current density, the faster the recovery rate. These recoveries are discussed below in connection with Equation 5.

We investigated next the influence of Pb substitution for Ru on the B sites of the $A_2B_2O_6O'_{1-y}$ structure. Figure 6 shows room-temperature polarization curves for $Pb_2Ru_{2-x}Pb_xO_{7-y}$ ($0.05 \leqslant x \leqslant 0.4$) electrodes with 5% Dow gel incorporated and bonded to a Dow membrane; all measurements were made with a 2.5 M H_2SO_4 reservoir solution. These curves illustrate dramatically that the electrode performance depends critically on x and exhibits a maximum near $x = 0.25$, the value used in the tests shown in Figs 2–5.

3.3.2. Oxide-on-treated-carbon electrodes. Figure 7 shows room-temperature polarization curves for two oxide electrodes on treated-carbon substrates with and without the incorporation of Dow gel and all bonded to a Dow membrane. The values of x in $Pb_2Ru_{2-x}Pb_xO_{7-y}$/C cannot be determined from the

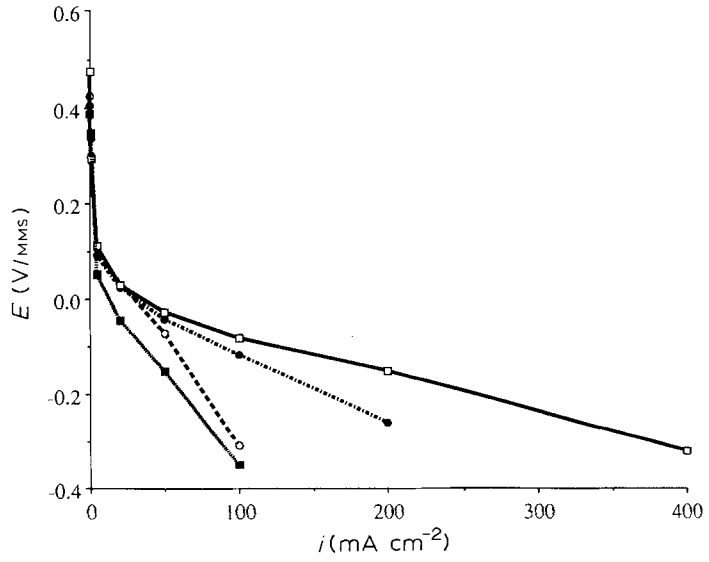

Fig. 6. Room-temperature performance curves for oxygen reduction on $Pb_2Ru_{2-x}Pb_xO_{7-y}$ (x = 0.05 to 0.4) with 5% Dow gel incorporated and bonded to a Dow membrane for a 2.5 M H_2SO_4 reservoir with p_{O_2} = 10 p.s.i. The data points were not iR-compensated. x values: (○) 0.05, (●) 0.17, (□) 0.26 and (■) 0.40.

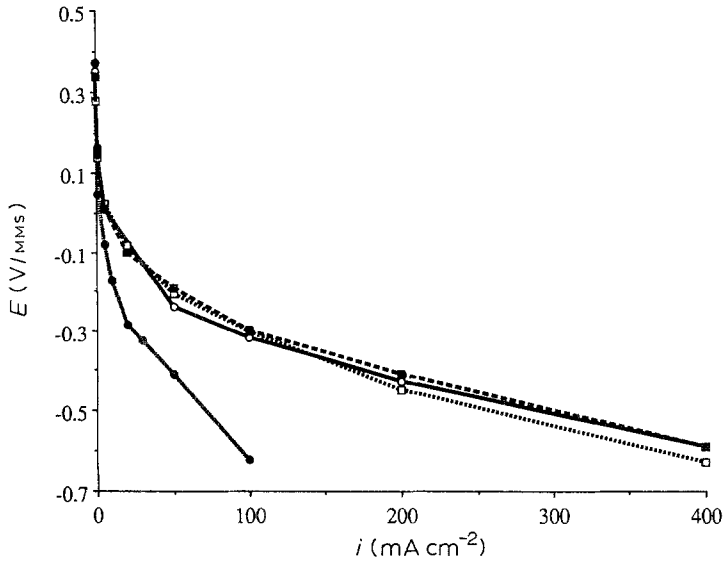

Fig. 7. Room-temperature oxygen-reduction polarization curves (without *iR*-compensation) for $Pb_2Ru_{2-w}Pb_wO_{7-y}$/C electrode (● and ○) and $Pb_2Ru_{2-z}Pb_zO_{7-y}$/C electrode (□ and ■) with a 2.5 M H_2SO_4 reservoir and p_{O_2} = 10 p.s.i. The symbols, in order, represent without and with 12% Dow gel. Also, $w > z$.

X-ray-diffraction lattice parameters because of the presence of the CO_2-treated vulcan XC-72 carbon. However, the starting molar ratios of Pb : Ru for the preparations of $x = w$ and $x = z$ were the same as those for $x = 0.35$ and 0.26, respectively, for the pure oxides, so we anticipate a $w \approx 0.35$ and $z \approx 0.26$ for the oxides precipitated on the carbon substrate. Addition of the carbon substrate gives no apparent improvement of the electrode performance; incorporation of the Dow gel clearly does. The cyclic voltammograms of Fig. 8, like those of Fig. 4, clearly show that the ORR is occurring on the oxides precipitated on the treated-carbon substrates. In the presence of nitrogen gas, the cyclic voltammogram of Fig. 8 shows the oxidation/reduction reaction of the surface Ru ions over a broad potential range. The differences in the shapes of the curves in Figs 4 and 8 are thought to be due to differences in the residual oxygen at the electrode in the two experiments. Greater resolution like that of Fig. 8 has been obtained on oxide catalysts prepared as those used in Fig. 4.

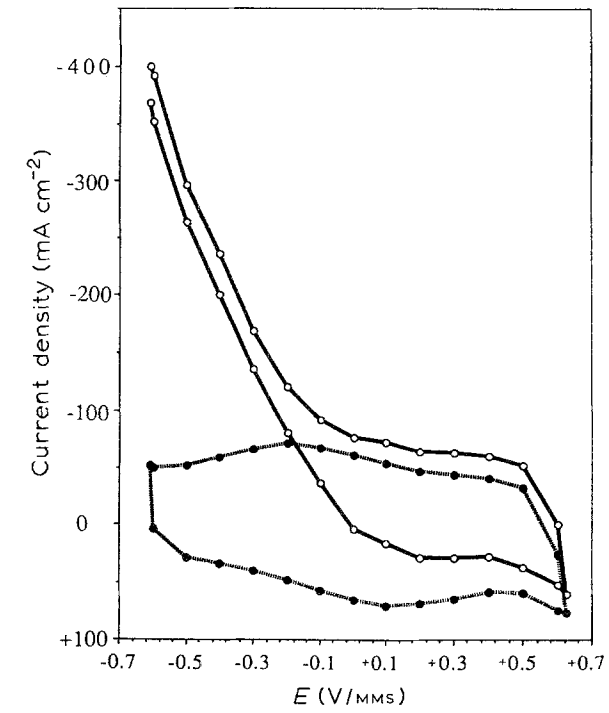

Fig. 8. Cyclic voltammograms for a $Pb_2Ru_{2-w}Pb_wO_{7-y}$/C electrode with 12% Dow gel incorporated and bonded to a Dow membrane with a 2.5 M H_2SO_4 reservoir and a scan rate of 100 mV s^{-1}; (○) p_{O_2} = 10 p.s.i., (●) p_{N_2} = 5 p.s.i.

3.4. *Bismuth-ruthenium oxides*

The performances of the $Bi_2Ru_{2-x}Bi_xO_{7-y}$ electrodes were similar to those of the $Pb_2Ru_{2-x}Pb_xO_{7-y}$ electrodes. Figure 9 shows curves for $Bi_2Ru_{1.6}Bi_{0.4}O_{7-y}$ and $Bi_2Ru_{2-x}Bi_xO_{7-y}$/C electrodes, where an $x \approx 0.4$ is anticipated for the oxide precipitated on treated carbon as the same starting molar ratio of Bi : Ru was used for both electrodes. Again, the incorporation of Dow gel dramatically improves performance, and the best performance is quite comparable to the performance for $Pb_2Ru_{1.74}Pb_{0.26}O_{7-y}$.

3.5. *Uncompensated resistance, R_u*

The uncompensated resistance R_u (Ωcm^{-2}) is the resistance per geometrical area measured perpendicular to the electrode with/without bonding to the Dow membranes. (Yes/No Dow membrane in Table 1). The thickness of the carbon sheet, the catalyst coating, and the proton-exchange membrane were, respectively, 0.35, 0.15, and 0.15 mm. The results for the several electrodes listed in Table 1 varied quantitatively. R_u is seen to increase with Teflon content, with the percentage of Dow gel incorporated, and with the concentration x of Pb substituted for Ru on the B sites of the pyrochlore structure; of course it also increases with the addition of the bonded Dow membrane. However, the measured variations in R_u are relatively small, which indicates that differences in R_u without the Dow membrane are not a controlling factor between the several performance curves of Fig. 6. On the other hand, a relatively large difference in the R_u for the two $Pb_2Ru_{2-x}Pb_xO_{7-y}$/C, $x = w$ against z, electrodes is directly reflected in the performance curves of Fig. 7.

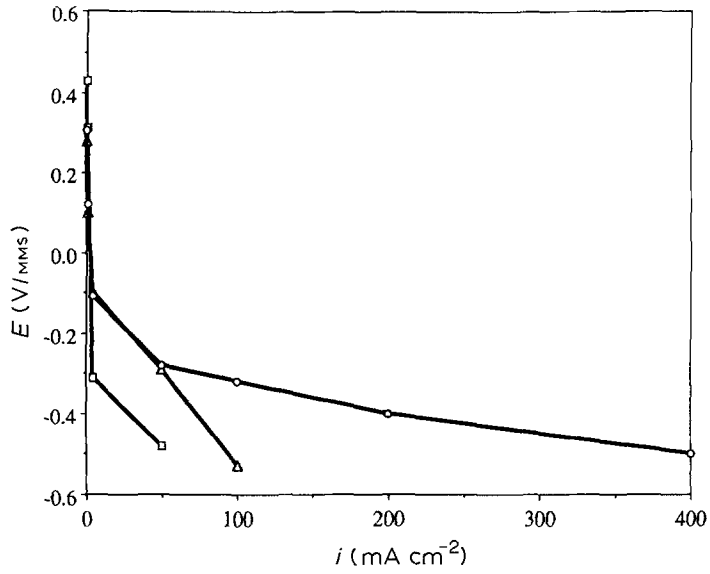

Fig. 9. Room-temperature oxygen-reduction polarization curves (without iR-compensation) for $Bi_2Ru_{1.6}Bi_{0.4}O_{7-y}$ (□, +0.6% Dow gel) and $Bi_2Ru_{2-x}Bi_xO_{7-y}$/C electrodes (△, +0.6% and ○, +12% Dow gel) obtained with a 2.5 M H_2SO_4 reservoir and p_{O_2} = 10 p.s.i.

3.6. *Surface charge density*

Figures 10 and 11 show the pH dependence of the mean surface charge density $\pm q_s$ on the oxide particles and the oxide-impregnated carbon particles, respectively. The values of q_s were calculated according to the standard procedure [18]:

$$\pm q_s = F\Delta V(C/S)W \qquad (1)$$

where F is the Faraday constant, ΔV is the difference in the volume of the titrant with and without the presence of the powder, C is the proton concentration of the titrant (pH 1.00 buffer solution), S is the BET surface area per gram ($m^2 g^{-1}$), and W is the weight of the powder used. The BET surface areas and the pH at which $q_s = 0$ (the p.z.z.p.) are given in Table 2.

4. Discussion

Interpretation of the data begins with the pyrochlore structure of the bulk oxides and the role of bound water at the oxide surface. The ideal structural formula $A_2B_2O_6O'$ contains a cubic B_2O_6 framework of corner-shared octahedra that is interpenetrated by an A_2O' subarray. The framework has its B–O–B bond angle buckled from 180° to about 135°. The O′ sites are tetrahedrally coordinated to just A cations; the O sites are coordinated to two A and two B cations. In $Pb_2Ru_{2-x}Pb_xO_6O'_{1-y}$, a $y \approx 0.5$ leaves half the O′ sites vacant; the A-site Pb^{2+} ions project lone-pair electrons into the oxygen vacancies. Substitution of Pb^{4+} ions for Ru on the B sites corresponds to a higher mean oxidation of the Ru atoms for a fixed value of y. In $Bi_2Ru_{2-x}Bi_xO_6O'_{1-y}$, a $y \approx 0$ is found for $x = 0$.

At high temperatures, the surface of an oxide particle may be reconstructed so as to complete the cationic preference for a full oxygen coordination; but if the oxide is precipitated in an aqueous solution, surface reconstruction is not required since the surface cations can bind the oxygen of water molecules [19]. Two consequences follow from this binding of surface

Table 1. Measured uncompensated resistance (R_u) for electrodes fabricated by different methods with a 2.5 M H_2SO_4 reservoir solution.

Electrode	x	*Teflon (w/w %)*	*Dow gel (w/w %)*	*Dow membrane*	R_u (Ωcm^{-2})
$Pb_2Ru_{2-x}Pb_xO_{7-y}$					
Teflon-bonded	0.40	22	0.6	no	6.70
without carbon	0.21	22	5	no	6.94
	0.17	22	5	no	6.56
	0.05	22	0	no	2.68
Teflon-bonded	w	25	0	no	5.00
with carbon	w	30	0	no	6.96
	w	22	0.6	no	5.80
	w	22	0.6	yes	11.30
	w	22	12	no	9.28
	w	22	12	yes	15.28
	z ($z < w$)	22	12	no	3.20
$Bi_2Ru_{2-x}Bi_xO_{7-y}$					
Teflon-bonded		22	0.6	no	6.56
with carbon		22	12	no	8.00
		22	12	yes	11.44

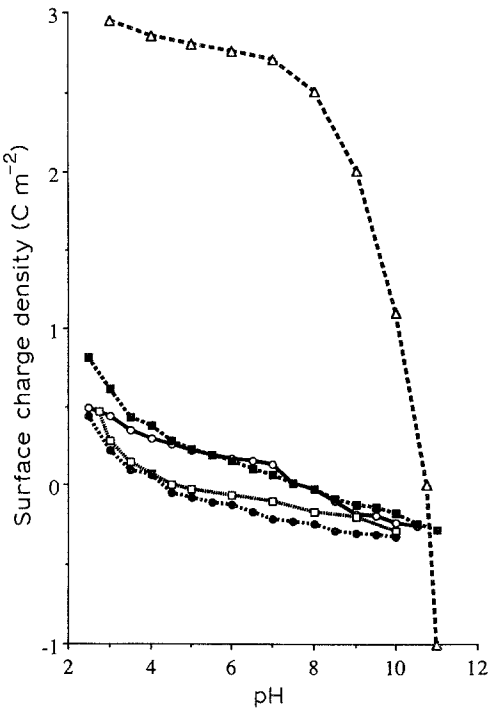

Fig. 10. Surface-charge densities of $Pb_2Ru_{2-x}Pb_xO_{7-y}$ (x = 0.1 to 0.4). All the data have been collected with a solution of constant ionic strength. x values: (△) 0 (from [6]), (○) 0.10, (□) 0.17, (●) 0.26 and (■) 0.40.

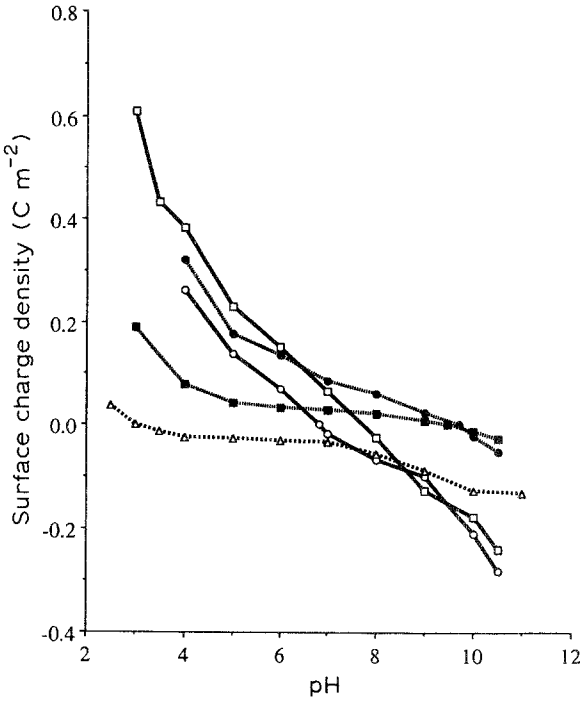

Fig. 11. Surface-charge densities of $Pb_2Ru_{1.6}Pb_{0.4}O_{7-y}$ and $Bi_2Ru_{1.6}Bi_{0.4}O_{7-y}$ with (● and ■) and without (□ and ○) CO_2-treated Vulcan XC-72 carbon in aqueous solution, respectively. Note: (△) CO_2 treated XC-72 alone.

water: (i) The surface of an oxide particle consists of oxygen species, so chemical reactions at an oxide surface are confined to those that involve the surface-oxygen species. (ii) Exchange of protons between the surface oxygen of the oxide particle and the oxygen of the aqueous ambient allows equilibrium to be established between the degree of surface protonation and the pH of the ambient solution. The pH of zero charge is a measure of the acid/base character of an oxide. For a given pH, the open-circuit voltage becomes shifted anodically (by donating surface protons) or cathodically (by accepting surface protons) on immersion of an oxide electrode into an aqueous electrolyte solution.

Given the constraint that chemical reactions at an oxide surface occur at surface-oxygen sites, the oxygen-evolution reaction (OER) would occur at the more acidic O-oxygen sites via the pathway [5, 6]

$$Ru^4OH^- \longrightarrow Ru^{5+}O^{2-} + H^+ + e^-$$

$$Ru^{5+}O^{2-} \rightleftharpoons Ru^{4+}O^-$$

$$Ru^{4+}O^- + H_2O \longrightarrow Ru^{4+}OOH^- + H^+ + e^- \quad (2)$$

whereas the rate-determining step near threshold (lower current densities) in the ORR in acid is the displacement reaction

$$Ru^{4+}OH^- + O_2H^{\cdot}_{ads} + e^- \longrightarrow Ru^{4+}OOH^- + H_2O \quad (3)$$

which also occurs at O-oxygen sites in acidic solution because the O′-oxygen sites are fully protonated to

Table 2. The BET surface area and the point of zero zeta potential (p.z.z.p.) for $Pb_2Ru_{2-x}Pb_xO_{7-y}$ and $Bi_2Ru_{2-x}Bi_xO_{7-y}$ with/without CO_2-treated Vulcan XC-72 carbon

	x	Carbon	Surface area ($m^2 g^{-1}$)	p.z.z.p. (pH)
$Pb_2Ru_{2-x}Pb_xO_{7-y}$				
	0.40	no	81	7.7
	0.26	no	71	3.9
	0.17	no	102	4.4
	0.10	no	70	7.6
	w	yes	381	9.5
$Bi_2Ru_{2-x}Bi_xO_{7-y}$				
	0.40	no	154	6.8
		yes	226	9.7

$O'H_2$ at lower pH. Measurements of the surface charge of the oxide particles against pH revealed that nearly full protonation of the O′-oxygen occurs before there is any appreciable protonation of the much more acidic O-oxygen. In fact, correlation of the pH of the peak overpotential, Fig. 3, with the pH below which significant protonation of the O-oxygen occurs provided the basis for suggesting that a shift in the displacement reaction from $Pb^{2+}O'H^-$ to $Ru^{4+}OH^-$ sites occurs at pH values where the reaction at O′ sites is blocked by the transformation of $Pb^{2+}O'H^-$ to $Pb^{2+}O'H_2$ species. We begin our discussion from the vantage point of this deduction.

The comparison in Fig. 3 of the overpotential at $5\,mA\,cm^{-2}$ against pH for $Pb_2Ru_{2-x}Pb_xO_{7-y}/C$ at 60°C in aqueous solution with that for $Pb_2Ru_{1.74}Pb_{0.26}O_{7-y}$ bonded to the Dow membrane at room temperature clearly shows a similar change in the active site with pH for both configurations. However, bonding to the Dow membrane is apparently equivalent to lowering the pH of the solution, so that with 2.5 M H_2SO_4 solution in the reservoir, the overpotential in acid is reduced to a value even below that obtained for the bare electrode in alkaline solution. Given the additional observation that the oxides are stable if bonded to the Dow membrane, it becomes clear that the lead-ruthenium and bismuth-ruthenium pyrochlores are competitive oxygen-reduction electrocatalysts if used with the Dow membrane.

As discussed elsewhere [5, 6], the pH of zero surface charge (p.z.z.p.) for the pyrochlore oxides varies sensitively with the occupancy of the O′ sites in the bulk; this occupancy determines the magnitude of $q_s > 0$ at the pH where all the O′ sites are occupied by $O'H_2$ species. (A $q_s = 0$ at this pH if all the surface O′ sites are vacant in the absence of bound water and the O-sites remain unprotonated.) The difference in the p.z.z.p. value obtained, Table 2, for the $Pb_2Ru_{2-x}Pb_xO_{7-y}$ and $Bi_2Ru_{2-x}Bi_xO_{7-y}$ oxides follows naturally from a $y \approx 0.5$ in the bulk of the former and a $y \approx 0.0$ in the bulk of the latter. The significant feature of Figs 10 and 11 is not the p.z.z.p., but the pH below which a marked increase in $q_s > 0$ sets in. This pH value correlates well with the maximum in the overvoltage versus pH observed in Fig. 3; at pH < 4, it is apparent that the more acidic O-oxygen atoms are being protonated to OH^- species. We therefore conclude that, as for ruthenium-oxide pyrochlores in aqueous solution, so also for ruthenium-oxide pyrochlores bonded to a Dow membrane the active site for the rate-determining step (r.d.s) shifts from an $O'H^-$ species to an OH^- species, and we may write the reaction pathway as

$$\begin{aligned} O_2 + e^- + H^+ &\longrightarrow O_2H^{\cdot}_{ads} \\ O_2H^{\cdot}_{ads} + BOH^- + e^- + H^+ &\xrightarrow{\text{r.d.s.}} BOOH^- + H_2O \\ BOOH^- + 2e^- + 2H^+ &\longrightarrow BOH^- + H_2O \end{aligned} \tag{4}$$

where the r.d.s. is a displacement of the O-site OH^- species. However, if this conclusion is correct, then we might expect the activity of the r.d.s. to depend upon the concentration x of non-ruthenium atoms on the B-cation sites.

The observation of an optimum B-site Pb concentration of $x \approx 0.26$ for the system $Pb_2Ru_{2-x}Pb_xO_{7-y}$ is consistent with this expectation; however, it forces us to ask next what roles the B-site Pb and Ru atoms are playing in the overall reaction.

Each O-oxygen – as distinguished from the O′-oxygen – is bonded to, at most, only two B cations. There are, therefore, five candidate O-oxygen sites: Ru–O_t, Pb–O_t, Ru–O_b–Ru, Ru–O_b–Pb, and Pb–O_b–Pb, where O_t is a terminal oxygen and O_b is a 135° bridging oxygen. As has already been noted by Beyerlein *et al.* [20], the strong Ru–O_b–Ru interactions within the B_2O_6 framework are responsible for the metallic conductivity of these pyrochlore oxides. Substitution of Pb or Bi into the B sites reduces the conductivity of the oxides, thereby increasing the resistance of the electrodes. We may conclude, therefore, that the B-site Ru atoms control the delivery of electrons to the surface and hence to the reaction sites. It follows that we may eliminate from consideration the O-oxygen sites Pb–O_t and Pb–O_b–Pb as well as the O′-oxygen. Moreover, the fact that the ORR is sensitive to x seems to imply that we can also eliminate the O-oxygen sites Ru–O_t and Ru–O_b–Ru. We therefore conclude that the most active site for the ORR is the bridging Ru–O_b–Pb oxygen site. There are two reasons why the Ru–O_b–Pb O-oxygen site would be the most active for a reaction requiring the displacement of an OH^- species. First, strong Ru–O π-bonding would tend to make a Ru–O_t site more acidic, and an unprotonated O_t, would be O_t oxygen more tightly bound than a protonated bridging oxygen. Second, the Pb–O_b–Ru bond is asymmetric; the Pb–O_b bond is primarily σ in character whereas the O_b–Ru bond has a strong π component. In addition, the formal valence on the Pb is fixed, at least in the bulk, as Pb^{4+} whereas that on the Ru may be either Ru^{5+} or Ru^{4+}. The OER commences at potentials anodic of the $Ru^{5+/4+}$ redox potential [5, 6] in accordance with Reaction 2, the ORR at potentials cathodic of this redox potential. Therefore, we may envisage a displacement reaction that proceeds as follows:

$$\begin{aligned} & \overset{H^-}{Pb^{4+}\text{–}O_b\text{–}Ru^{4+}} + O_2H^{\cdot}_{ads} \\ &\longrightarrow Pb^{4+} \cdots \overset{O_bH^-}{\underset{O_2H^-}{>}} Ru^{5+} \\ &\xrightarrow{e^- + H^+} Pb^{4+}\text{–}O_b\text{–}Ru^{4+} + H_2O \end{aligned} \tag{5}$$

In Fig. 5, the rates at which the potential reaches its equilibrium value, after switching the current, increases as the potential becomes more negative. Since the displacement Reaction 5 requires charge transfer from a Ru^{4+} ion at the surface to an adsorbed $O_2H^{\cdot}$ species, this observation would imply that the

Fermi energy level lies below the $Ru^{5+/4+}$ couple for a surface ruthenium bridging to a Pb^{4+} ion at the rest potential. On switching off the current, recovery is more rapid when the value of the current is higher because the surface concentration of intermediates is higher. Restoration of the surface requires a surface diffusion of active oxygen to form O_2 gas; and the greater the concentration of active intermediates, the shorter is the diffusion pathway for dioxygen formation.

Similar arguments for the $Bi_2Ru_{2-x}Bi_xO_{7-y}$ oxides would identify the Bi–O_b–Ru O-oxygen site as the most active in acid for the ORR on these pyrochlore oxides. The fact that the activities of the lead-ruthenium and bismuth-ruthenium pyrochlore oxides are comparable in acid for the membrane-bonded electrodes is consistent with this interpretation.

The data of Fig. 10 require further consideration. The sample prepared at high temperature has no B-site Pb^{4+} ions ($x = 0$) and a chemical formula $Pb_2Ru_2O_6O'_{0.5}$ [21]. For such a composition, all the surface oxygen vacancies are at O′ sites and the oxide particle is neutral ($q_s = 0$) if all the O′-site vacancies are occupied by H_2O and none of the surface oxygen are protonated. Of course, in an aqueous medium at the pH of zero charge, the protons become distributed equally over all the O′ oxygen as $O'H^-$ species. This situation means that protonation of the O′ sites to $O'H_2$ charges the particles positively ($q_s > 0$) as is found experimentally, Fig. 10. It is therefore interesting to note a remarkable shift of the q_s against pH curves toward more negative q_s values with increasing x in $Pb_2(Ru_{2-x}Pb_x)O_6O'_{1-y}$ for $0 \leqslant x \leqslant 0.26$. If y increases with x at the surface, at least part of the shift could be accounted for. However, measurement of the bulk value $y = 0.5$ for all x has been reported [7], so it is necessary to look for some other explanation. We therefore argue that the surface B–site Pb atoms influence significantly the q_s against pH curves.

The fact that the pH of zero charge has a minimum value near $x = 0.26$ where the activity is highest is consistent if the O_b oxygen bridging B-site Pb and Ru is more acidic than an O_b bridging either two Pb or two Ru atoms. A more acidic O_b means that the oxygen is more tightly bound to the Ru atom, which allows for initiation of the displacement reaction. A shift of O_b from Pb toward Ru would make the Ru–O_b bond approach that of a Ru–O_t bond, and the O_t oxygen is characteristically more acidic than an O_b oxygen where the cation allows for strong π backbonding.

Precipitation of the oxide onto a treated-carbon substrate appears to have little influence on the activity of the electrode in 2.5 M H_2SO_4. Nevertheless, the data of Figs 10 and 11 give indirect evidence for electron transfer from the oxide to the substrate. In Fig. 11, the q_s against pH curve for the pure treated-carbon substrate is shifted to a more positive q_s on impregnation of the substrate with the oxide; moreover, the curve is also shifted to a more positive q_s relative to its value for the bare oxide at pH values > 6.5. This result is consistent with the arguments of the above paragraph if electrons are transferred from the oxide to the treated-carbon substrate. Reduction of the substrate would be balanced by protonation of the substrate; oxidation of the oxide would be balanced by an effective reduction in the O′-vacancy concentration y.

Finally, Fig. 3 indicates that the acidic character of the membrane effectively lowers the pH at an electrode bonded to the membrane relative to a given reservoir solution pH, but it does so without corroding the electrode because the anions at the electrode surface are immobile.

5. Conclusions

The following conclusions result from this study:

1. The pyrochlore ruthenium oxides $Pb_2Ru_{2-x}Pb_xO_{7-y}$ and $Bi_2Ru_{2-x}Bi_xO_{7-y}$ catalyze the ORR in both acid and alkaline environments, but the active site for the r.d.s. changes with pH.

2. Although these oxides are not stable by themselves under a cathodic load in an acidic aqueous solution, they are stable if bonded to a Dow membrane — and presumably to any solid-polymer proton-exchange membrane — that is exposed to an aqueous electrolyte reservoir on the opposite side of the membrane.

3. Given the change in the active site — from an $O'H^-$ species at a more basic O′-oxygen site in alkaline solution to an OH^- species at an O-oxygen site in more acidic solutions — the stronger the proton activity at the catalyst surface, the greater the activity. It follows that a more acidic polymer should have a greater ORR activity for a given reservoir solution pH.

4. Substitution of Pb or Bi for Ru on the B sites enhances the ORR up to an optimum concentration, and the most active site in acid appears to be a bridging O-oxygen site Pb–O_b–Ru or Bi–O_b–Ru.

5. The presence of a $Ru^{5+/4+}$ redox couple between the potentials for the OER and the ORR and Ru–O_b–Ru interactions strong enough to make the oxide metallic appear to play critical roles in rendering the ruthenium oxides active to these two reactions.

6. Electrode fabrication is critical to electrode performance. (a) More than 15% by weight Teflon is required to obtain good electrode porosity and binding of the electrode particles; more than 25% by weight Teflon isolates the electrode particles. We found about 22% by weight Teflon to be optimal for our electrodes. (b) Incorporation of Dow gel — we found about 5% by weight of the oxide weight for 22% by weight Teflon to be nearly optimal — enlarges the reactant-catalyst-electrolyte three-phase interface area and provides improved bonding to the Dow membranes. (c) Precipitation of the oxide onto a CO_2-treated Vulcan XC-72 carbon substrate increases the catalytic surface area for a given catalyst loading. (d) The electrode-electrolyte interface resistance

becomes an important parameter for electrode performance at higher current densities.

7. Although there is evidence of electron transfer from the oxide to the substrate for electrodes consisting of pyrochlore oxides on treated-carbon substrates, nevertheless there appears to be little difference in electrode performance in 2.5 M H_2SO_4 between electrodes with/without a treated-carbon substrate.

8. The stability and activity of the ORR on ruthenium-oxide pyrochlores that are bonded to a Dow membrane are sufficiently encouraging at room temperature to warrant development and testing of these systems for operation at 60–100° C in an operative fuel cell.

After communicating this paper, we came to know that Jai Prakash *et al.* have independently stabilized the pyrochlore oxides with anionically conducting polymer layers in alkaline electrolyte [22].

Acknowledgments

We thank the Dow Chemical Company for supplying the Dow membrane material and Dow gel used in this study and for financial support of the project. The assistance of Dr M. Paranthaman with surface-charge measurements is gratefully acknowledged. Drs A. Cisar and G. Eisman of the Dow Chemical Company supplied the electrochemical cell used in this study, and we are grateful for their cooperation and encouragement.

References

[1] H. S. Horowitz, J. M. Longo and J. T. Lewandowski, *US Patent* 4 129 525 (1978).
[2] R. Manoharan, A. Hamnett and J. B. Goodenough, in 'Book of Abstracts' of the Third European Conference on Solid State Chemistry, Vol. 2, Regensburg (1986) p. 226.
[3] G. A. Eisman, *Proc. Electrochem. Soc.* **86** (1986) 13, 156.
[4] D. Chu, D. Gervasio, M. Razaq and E. B. Yeager, *J. Applied Electrochem.* **20** (1990) 157.
[5] R. Manoharan, M. Paranthaman and J. B. Goodenough, *Eur. J. Solid State Inorg. Chem.* **26** (1989) 155.
[6] *Idem, J. Amer. Chem. Soc.* **112** (1990) 2076.
[7] H. S. Horowitz, J. M. Longo, H. H. Horowitz and J. T. Lewandowski, in 'Solid State Chemistry in Catalysis' (edited by R. K. Grasselli, and J. F. Brazdil), ACS Symposium Series 279 American Chemical Society, Washington, DC (1985) p. 143.
[8] R. Manoharan, J. B. Goodenough and A. Hamnett, *J. Appl. Electrochem.* **17** (1985) 413.
[9] S. J. Ridge, R. E. White, Y. Tsou, R. N. Beaver and G. A. Eisman, *J. Electrochem. Soc.* **136** (1989) 1902.
[10] H. Kita, N. Henmi, K. Shimazu, H. Hattori and K. Tanabe, *J. Chem. Soc., Faraday Trans.* **1** (1981) 77, 2451.
[11] G. A. Parks, *Chem. Rev.* **65** (1965) 177.
[12] J. W. Murray, *J. Colloid Interface Sci.* **46** (1954) 357.
[13] D. N. Furlong, D. E. Yates and T. W. Haeley, in 'Electrodes of Conductive Metallic Oxides', (edited by S. Trasatti), Elsevier, New York (1981).
[14] R. J. Atkinson, A. M. Posner and I. P. Quirk, *J. Phys. Chem.* **71** (1967) 550.
[15] J. W. Bowden, M. D. A. Bollard, A. M. Posner and J. P. Quirk, *Nature* **245** (1973) 81.
[16] A. J. Appleby and E. B. Yeager, *Energy* **11** (1986) 137.
[17] A. K. Shukla, P. Stevens, A. Hamnett and J. B. Goodenough, *J. Appl. Electrochem.* **19** (1989) 383.
[18] J. O'M. Bockris and T. Otagawa, *J. Electrochem. Soc.* **131** (1986) 290.
[19] W. A. England, M. G. Cross, A. Hamnett, P. J. Wiseman and J. B. Goodenough, *Solid State Ionics* **1** (1980) 231.
[20] R. A. Beyerlein, H. S. Horowitz and J. M. Longo, *J. Solid State Chem.* **72** (1988) 2.
[21] R. A. Beyerlein, H. S. Horowitz, J. M. Longo, M. E. Leonowicz, J. D. Jorgensen and F. J. Rotella, *ibid.* **51** (1984) 253.
[22] Jai Prakash *et al. J. Power Sources,* **29** (1990) 413.